Development and investigation of a high melting point binary sodium salt based composite phase change thermal energy storage material by an ultra-low sintering temperature with cold sintering technique

Guofeng Wei [a,b], Dehao Xiu [c]*, Yanping Du [d], Chuan Li [a,c], Geng Qiao [e]*, Qi Li [a,c]*

[a] BJUT-CQOB joint lab for energy storage and utilization, Beijing University of Technology, Beijing, 100124, China

[b] The First Gas Production Plant of China Petroleum Changqing Oilfield Branch, Jingbian, 718500, China

[c] College of Mechanical and Energy Engineering, Beijing University of Technology, Beijing, 100124, China

[d] School of Engineering, Lancaster University, Lancaster LA1 4YW, UK

[e] Global Energy Interconnection Research Institute Europe GmbH, 10117 Berlin, Germany

*Corresponding authors: xiudehao@bjut.edu.cn (D Xiu); Geng.Qiao@geiri.eu (G Qiao); liqi@bjut.edu.cn (Q Li);

Abstract

This work focuses on the development of a high melting point binary sodium salt phase change composite by an ultra-low sintering temperature for thermal energy storage. A so-called cold sintering approach is used for the composite fabrication in which a eutectic salt of Na_2SO_4/NaCl is adopted as phase change substance and diatomite is employed as skeleton material. By using sodium hydroxide solution as sintering agent, the effects of operation conditions and ingredient composition on the composite microstructural characteristics, mechanical and thermophysical properties as well as thermal stability are evaluated. The results indicate that the salt-diatomite composite could be successfully fabricated by a sintering temperature as low as 150 °C. A shape-stabilized framework containing a compact and dense microstructure could be obtained in the composite with the use of aqueous alkali as sintering liquid. Splendid chemical and physical compatibility have also been attained among the ingredients of sodium salt, diatomite and aqueous alkali. For a given uniaxial pressure, a mechanical strength as high as 253.84MPa could be achieved in the composite. Over 60% of salt could be encapsulated by diatomite without the occurrence of liquid divulge. At such a composition, the composite presents a melting point of 623.9 °C and a latent heat of 148.2kJ/kg. Moreover, the composite also exhibits excellent cycling performance and after experienced 300 heating-cooling cycles, a perfect macroscopic shape could be maintained and the latent heat of the composite only changes 4.9%, demonstrating the composite prepared through cold sintering technique in this work can be a competitive candidate used in medium and high temperature fields.

Keywords: Binary sodium salt; Shape stabilization; Cold sintering; Thermal energy storage; Phase change material

1. Introduction

As one of competitive phase change substances for heat energy storage applications, molten salts have been widely utilized in numerous fields including solar thermal power generation, waste heat

recovery and sea water desalination owning to its merits of suitable operating temperature range, high heat storage density, high stability and low budget [1-3]. A number of salts involving single or multiple phases have been explored and reported in the literatures [4, 5]. These materials present different thermophysical properties and hence exhibit various drawbacks such as chemical incompatibility, poor thermal conductivity and low heat capacity as well as liquid leakage [4, 6].

A multitude of methods have been developed to overcome these defects, which is comprised of formation of matrix to address liquid divulgence, addition of enhancer to improve effective thermal conductivity and generation of capsules to limit and alleviate corrosion [6-9]. Among these approaches, the development of ceramic based shape-stable salt composite is reported to be able to resolve the limitations faced by salts simultaneously [10, 11]. For fabrication of such salt composites, a so-called hot sintering technique is usually adopted through the selection of suitable skeleton ceramic material for structure supporting and high-thermal conductivity agent for performance enhancement [12, 13]. Li et al. [14] developed a ternary chloride salt phase change composite by adopting hot sintering approach. A rice husk carbon together with MgO and expanded graphite particles is adopted as skeleton structure material to accommodate chloride salt. They reported that the rice husk carbon with an in-situ SiO_2-C interconnected structure could act as not only the structure supporting substance, but also the thermal conductivity enhancer. Over 65 wt.% of phase change substance is effectively encapsulated in the composite without the occurrence of liquid leakage over the charging and discharging processes. 20 wt.% MgO-10 wt.% rice husk carbon-10 wt.% expanded graphite was the optimal formation for the skeleton supporting material, and with the use of such a formulation, the composite thermal conductivity can reach 8.86 W/m·℃. In addition, the composite also exhibited splendid thermal cycling performance. After 1000-time thermal cycles, the composite enthalpy loss was only 8.5%. Yao et al. [15] fabricated a novel metallic microcapsule/molten salt composite with the adoption of hot sintering method. By using MgO particle as structure material, the composite thermophysical properties and also the feasibility of composite fabrication through the use of metallic microcapsule instead of MgO are evaluated. Due to the similar phase change range, the microcapsule of Sn@void@SiO_2 can also be used as phase change material and hence improve the composite overall heat storage density. It was found that the composite achieved the best performance by using 30 wt.% metal microcapsule replacement of MgO, and at this ratio, the composite latent heat was measured as 117.9 J/g. In addition, the composite thermal conductivity could also be improved by 64% increasing from 0.58 W/m·℃ to 0.95 W/m·℃. Later, the same team [16] also adopted hot-sintering method to explore the performance enhancement in the Sn@void@SiO_2/MgO/$LiNO_3$-NaCl composite by doping of graphene, carbon fibre and Sn. It was revealed that a thermal conductivity over 2.1 W/m·℃ could be attained by addition of 3 wt.% graphene and 2 wt.% Sn, which was increased by 128% in comparison with pure salt. Owning to the existence of SiO_2 nanoparticles, the composite heat capacity can also be improved, and they reported that 1 wt.% SiO_2 resulted in 8.9% increase in the sample heat capacity. By employing hot sintering technique, Liu et al. [17] prepared a $MgAl_2O_4$ composite and investigated the influence of particle packing structure on the salt migration behaviour. With the use of NaCl-KCl as phase change substance, their results indicated that a decrease of ceramic particle size achieved an improvement of composite thermal stability and mechanical performance due to the limitation of salt migration and evaporation that caused by decreased vapour pressure and increased capillary pressure. When the $MgAl_2O_4$ particle size is less than 0.01 mm, the mass loss of the composite can be reduced by 72.3% and the compressive strength

value can reach 48 MPa. Our previous work [18] also used hot sintering method to produce a salt/vermiculite/SiC composite and found that owning to the decent wettability of ceramic substance in liquid salt, a dense and rigid structure with numerous micropores was formed in the composite. Such a structure offers spaces to contain the salt and prevents the liquid divulgence over heating-cooling cycles.

Analysing above-mentioned literatures, it can be found that even through the use of hot sintering technique could be able to endow the salt composite with splendid thermal and mechanical properties, it is usually highly energy-consuming and time-consuming since a sintering duration longer than several hours or even more and a higher operation temperature than the salt melting temperature are typical required. Such high-temperature conditions can not only induce the occurrence of chemical reaction among the ingredients but also bring about cumbersome operations for the whole fabrication process. Recent investigations have indicated that the employment of a so-called cold sintering technique provides a solution for these challenges [19, 20]. In such a technique, the densification and sintering of ceramic could be occurred at a quite low temperature usually less than 200 °C and a short time (minute level) through the selection of appropriate sintering liquid and mechanical pressure [21, 22]. Yu et al. [23] studied a $NaNO_3$-$Ca(OH)_2$ composite through the cold sintering method. By using deionized water as sintering additive, they reported the occurrence of particle rearrangement-precipitation process in the composite over the material fabrication process. Owning to such a phenomenon, a rigid structure with apparent sintered boundaries could be formed, which could effectively encapsulate the salt and supress the liquid divulge. By employing the same fabrication technique, Suleiman et al. [24] reported the development of a chloride salt composite containing Al_2O_3 as skeleton material and water as sintering liquid. Because of the solubility of aluminium oxide in chloride salt solution, a sintered structure was generated over the preparation process, which could effectively retain the salt without the occurrence of leakage even experienced 30 heat-cold cycles. Similarly, Liu et al. [25] also explored the adoption of water as sintering agent to fabricate nitrate salt composite with the same technique, and they found that the ceramic material could encapsulate the salt to form a rigid structure in the composite.

Although the cold sintering technique presents a huge advantage in the salt composite fabrication, relatively little works are available in the literatures and there is a considerable research space remained on this subject particular for the choice of suitable sintering additives apart from deionized water that soluble with different ceramic substances and fabrication of salt based composites with high melting temperatures above 500 °C. Besides that, the detailed effect of sintering operation conditions on the composite thermal performance also requires to be explored. This work makes a contribution to fill such research gap in which a chloride salt based composite with melting temperature above 600 °C is fabricated and investigated by cold sintering technique through the utilization of diatomite as structure ceramic and aqueous alkali as sintering liquid. Specifically, the impacts of operating conditions including uniaxial pressure, sintering temperature, duration and sintering liquid concentration on the composite density are first evaluated to ascertain the optimal sintering parameters. The composite microstructural characteristics and chemical compatibility as well as thermal stability are then investigated. Finally, the phase change behaviour and heat storage performance of the composite are determined. The results confirm the preparation feasibility of a high melting point salt composite by an ultra-low sintering temperature with cold sintering technique and demonstrate the splendid energy storage performance of the salt-diatomite composite that could be a promising alternative utilized in high-temperature heat energy storage fields.

2. Materials and method

2.1. Raw materials

A mixed sodium salt of Na_2SO_4/NaCl is used as PCM in this work in which sodium sulphate is obtained from Shanghai Yien Chemical Technology Co., Ltd., and sodium chloride is got from Shanghai Aladdin Biochemical Technology Co., Ltd. Both of these materials have a purity greater than 99% and a mean particle size less than 5 μm. Diatomite with a median particle size of 40 μm is adopted as skeleton material and obtained from Shanghai Maclean's Biochemical Technology Co., Ltd. Sodium hydroxide is of analytical grade and got from Shanghai Aladdin Biochemical Technology Co., Ltd. Deionized water is produced by a deionizer in our laboratory. All these raw materials are used directly over the composite fabrication process without any treatments.

2.2. Preparation of binary eutectic salt

The binary sodium salt of Na_2SO_4/NaCl is first prepared prior to the composite fabrication. Specifically, the raw materials of Na_2SO_4 and NaCl with a ratio of 68:32 are weighed up by using an electronic balance, followed by fully mixing at a ball grinder at a speed of 300 rpm for 30 min. Then the mixed salts are transferred to a ceramic crucible and placed into a muffle furnace to melt. The heating procedure is as follows: heating from 20°C to 125°C at a rate of 10°C/min, and keeping at a temperature of 125°C for 30 min to remove the residual moisture in the sample; heating further from 125°C to 650°C at a rate of 10°C/min and maintaining for 60 min to assure complete melting of the binary salts. After that, the prepared binary salts are cooled down to room temperature with a temperature-controlled program that completely opposite to the heating process. The obtained sample is finally ground into powder state using a ball mill, and placed in a blast drying oven for further experiments.

2.3. Preparation of salt-diatomite phase change composite

A typical cold sintering technique is adopted for the fabrication of the salt-diatomite composite and the specific preparation process is shown in Fig. 1. More details for this sintering approach can refer to our previous publications [19, 20]. In this work, briefly, the process can be categorised into the following three steps. First, the binary salt and diatomite are accurately weighed using an electronic balance with a mass ratio of 6:4, and followed by blending the mixture into a ball mill for 30 min with a speed of 500 rpm. Secondly, a preset amount of sodium hydroxide solution is equably added into the mixed sample by using a sprayer, followed by further blending the mixture for 60 min at a speed of 200 rpm and then transferring the well-mixed sample to the stainless-steel heating mould; Finally, the salt composite is sintered using a temperature-controlled press apparatus under a pressure of 150 MPa and a temperature of 150 °C. Through repetitive the operation conditions different samples can be obtained. All the composites are stored into a blast drying oven for further testing and characterization.

Fig. 1. Preparation process for the salt-diatomite composite phase change materials using cold sintering technique.

2.4 Characterizations

The sample chemical compatibility and stability is measured by an X-ray diffractometer (XRD, D8 Discover, Bruker, Germany) and Fourier transform infrared spectrometry (FTIR, INVENIO-S, Bruker, German). Scanning electron microscopy (SEM, sigma 300, Zeiss, German) is used to observe the microscopic features of the composite. A self-designed high-temperature heating and cooling cycling facility covering a temperature range of 20-1000 °C is adopted to evaluate the sample cycling performance. Differential scanning calorimetry (DSC, DSC 404 F3, Netzsch, German) is employed to measure the sample phase transition behaviours. A thermogravimetry/differential thermal integrated analyser (TG, TG/DTA 7300, HITACHI, Japan) is employed to measure decomposition temperature of the composite, and a universal testing machine (CMT5105, MTS, USA) is used to explore the mechanical strength of the composite by using a loading rate is 0.2mm/min. The relative density of the sample is calculated with the use of the actual density dividing to the theoretical density, the actual density is measured by the geometric method, and the theoretical density is determined using the following equation [19, 25].

$$\rho = \frac{(M_1 + M_2)}{(\frac{M_1}{\rho_1} + \frac{M_2}{\rho_2})} \times 100\%$$

where M_1 and M_2 respectively are the weights of the diatomite and sodium salt; ρ_1 *and* ρ_2 respectively represent densities of the diatomite and sodium salt.

3. Results and Discussions

3.1. Influence of sintering parameters on composite density

To figure out the impact of operation conditions on the composite performance and also the optimum sintering parameters for the composite fabrication, the relative density of the composite is evaluated under various sintering parameters including uniaxial pressure, sintering additive concentrations, sintering duration and temperature. Fig. 2 plots the measurement results. It is seen that for different mass ratio of sintering agent, the sample relative density maintains growth over the selected sintering agent range of 5%-13%, as illustrated in Fig. 2 (a). It seems that the composite density has a linear relation with the sintering agent concentration. When a low mass ratio of sintering agent is involved, the binary sodium salt and diatomite particles cannot be completely moistened, which limits the particle rearrangement over the cold sintering process, and hence a low-density value is obtained in the composite. However, when a high proportion of sintering liquid is added, the salt and diatomite particles would be immoderately wetted, leading to the generation of excessive pores and caves during the moisture evaporation and thus an adverse impact on the composite microstructure and density. Our previous work has also indicated the occurrence of reaction between the diatomite and sodium hydroxide [19]. In the case of sodium hydroxide content is too large, the reaction between sodium hydroxide and diatomite will become violent, causing the increase of sodium silicate in the composite. This will lead to a reduction in the heat storage density of the composite. In this investigation, the composite relative density has been over 95% when the sintering concentration is 7%, so the sintering mass ratio is set as 7% in the following experiment. Fig. 2 (b) shows the variation of sample density with sintering duration. It can be seen that the density value fluctuates with the increase of sintering duration. When the sintering time is increased to 12 min, the composite density exceeds 95% and the further change of sintering duration has no apparent impact on the sample density. This hints that the densification rate of particles is rapid and the rigid structure in the composite is formed in a very early time during sintering. In Fig. 2 (c), the influence of sintering temperature is drawn. One thing to note is that over the cold sintering process, the uniaxial pressure and heating temperature are given simultaneously to reduce the impact of evaporation and therefore in this investigation, the fabrication is completed by warming-up the mould to the required temperature first and then implementing uniaxial pressure for cold sintering. It is seen from the figure that the composite density increases with sintering temperature first from 90 °C to 120 °C and reaches up to a peak value at 120 °C. This is because that a low sintering temperature cannot provide sufficient thermal tractive force for the diatomite grain boundary migration, resulting in a low composite density. On the other hand, when the sintering temperature is too high, the evaporation rate of the sintering agent becomes fast, which limits the rearrangement of particles, and thus causing a low sample density. Shown in Fig. 2 (d) is the measured curve for the influence of uniaxial pressure. It can be seen that the composite relative density is increased with the increase of uniaxial pressure when the uniaxial pressure is less than 150MPa. At such a pressure, the composite density has surpassed 95%. In the case of pressure value is higher than 150 MPa, the value of the composite density is maintained around 95%. The main reason for this observation is that the uniaxial pressure as one of the major parameters affects particle arrangement and transport over the densification process. The high solubility at a fixed high uniaxial pressure helps to wet the particles and pull them movement and arrangement to achieve initial densification. Based on these analyses, it can be summarized that the optimal cold sintering parameters for the material fabrication in this work are 7 wt.% on sintering additive, 150 MPa on pressure, 120 °C on sintering temperature and 12 min on sintering time. Unless specified otherwise, the samples mentioned later are all fabricated by using these cold sintering parameters.

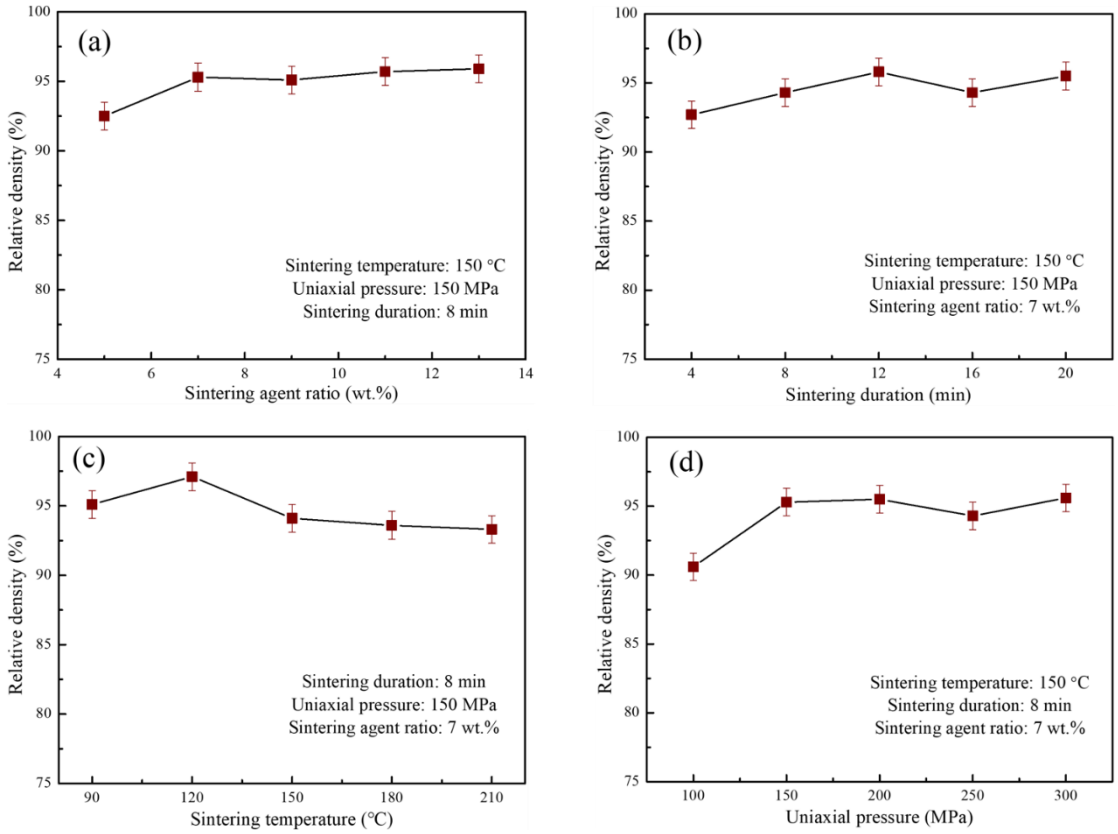

Fig. 2. Effects of cold sintering operation parameters on the composite density: (a) Sintering agent ratio; (b) Sintering duration; (c) Sintering temperature; (d) Uniaxial pressure.

3.2. Chemical stability and compatibility

Both X-ray diffraction and Fourier transform infrared spectroscopy are adopted to explore the chemical and physical compatibility within the composite. Fig. 3 plots the XRD results and it can be seen that six major diffraction peaks of 26°, 32°, 46°, 53°, 57°, and 76° are apparent in the pure sodium salt; see Fig. 3 (a). For diatomite, there are two main peaks at 2θ=21.5° and 36° observed with some inconspicuous peaks concentrated on the peaks between 27° and 31°, as illustrated in Fig. 3 (b). Blending of salt into diatomite makes no difference on the material chemical structure. For the composite, as showed in Fig. 3 (c), all characteristic peaks are in accordance with these appeared in the pure materials, demonstrating preeminent chemical compatibility has been attained in the composite even experienced pressure and sintering process. Shown in Fig. 3 also has the result for the sample after 300 thermal cycles. One can see that the main diffraction peaks displayed in the samples after 300 cycles and one cycle bring into correspondence with each other, indicating there is no new chemicals generated over repetitive heating and cooling processes and confirms the chemical compatibility of the components of salt, diatomite and sintering additive in this work. It is needed to point out here that our previous investigation has reported a good chemical stability among the nitrate salt-diatomite- aqueous alkali composite [19]. For the composite containing a low concentration of aqueous alkali, the slight reaction is occurred on the diatomite particle surface, contributing to the taking place of dissolution-precipitation process and formation of bonded skeleton structure during the cold sintering period. Such slight reaction is the main driving force for the congruent solubility of diatomite and salt in aqueous alkali, and also the key reason for

successful preparation of the diatomite-salt composite by cold sintering approach.

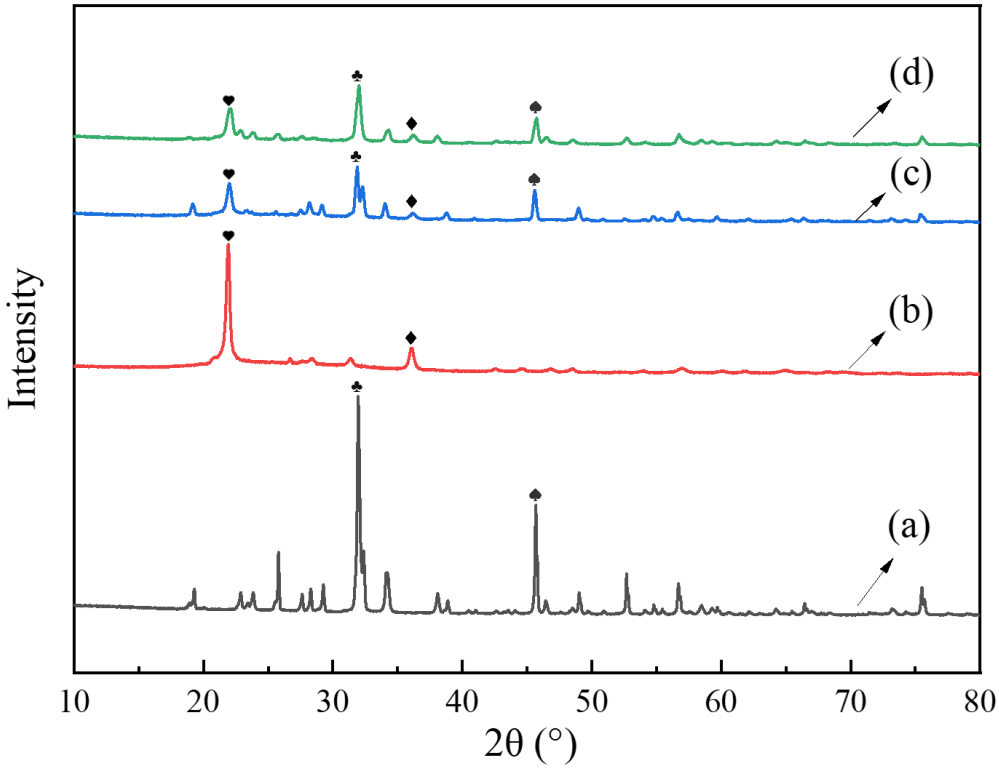

Fig. 3. XRD measurements for the tested samples: (a) Binary eutectic salts; (b) Diatomite; (c) Salt-diatomite composite; (d) Salt-diatomite composite after 300 heat-cold cycles.

The FT-IR analyses on the samples are depicted in Fig. 4. It is seen that the main absorption peaks of pure eutectic salts respectively appear at 640cm^{-1}, 992cm^{-1}, 1139cm^{-1} and 3441cm^{-1}. The first peak is caused by the superposition of NaCl lattice vibration and O-S-O bending vibration, while the second one is attributed to the symmetrical telescopic vibration of S-O. The peak of 1139cm^{-1} is related to the asymmetric telescopic vibration of S-O. Due to the unavoidable water absorption, part of the moisture in the air is absorbed by the samples during the experiment, and a vibration peak of -OH at 3441 cm^{-1} is therefore distinct. For diatomite, there are three major peaks of 467 cm^{-1}, 797 cm^{-1}, and 1083 cm^{-1} appeared, which is in line with the investigations reported by Moulakhnif et al. [26], as shown in Fig. 4 (b). These peaks are respectively attributed to the bending, symmetric, and asymmetric extension vibrations of the Si-O-Si bonds. Mixing of salt with diatomite does not result in any change to the peaks arose in the pure samples. As denoted in Fig 4 (c), no new peaks are emerged during the measurements, demonstrating a stabilized chemical structure in the salt-diatomite sample. Fig. 4 (d) shows the result for the composite experienced 300 thermal cycles. One can see that no new substance or bond is found and almost the same spectrums with that of composite after cold sintering are observed, further revealing the outstanding chemical compatibility achieved in the composite. However, it is important to point out here that although the synergistic dissolution of salt and diatomite in sodium hydroxide solution is the major driver for the particle precipitation and rearrangement, there will be existence of distinct chemical reaction in the diatomite-salt system diatomite in the case of aqueous alkali concentration is high [19]. In this work, only 7 wt.% of aqueous alkali is used as sintering additive and such a loading ratio can not only induce the occurrence of slight reaction on the diatomite surface to contribute to completion of the

dissolution-precipitation process, but also avoid the formation of a great deal of sodium silicate to influence the composite energy storage density and capacity.

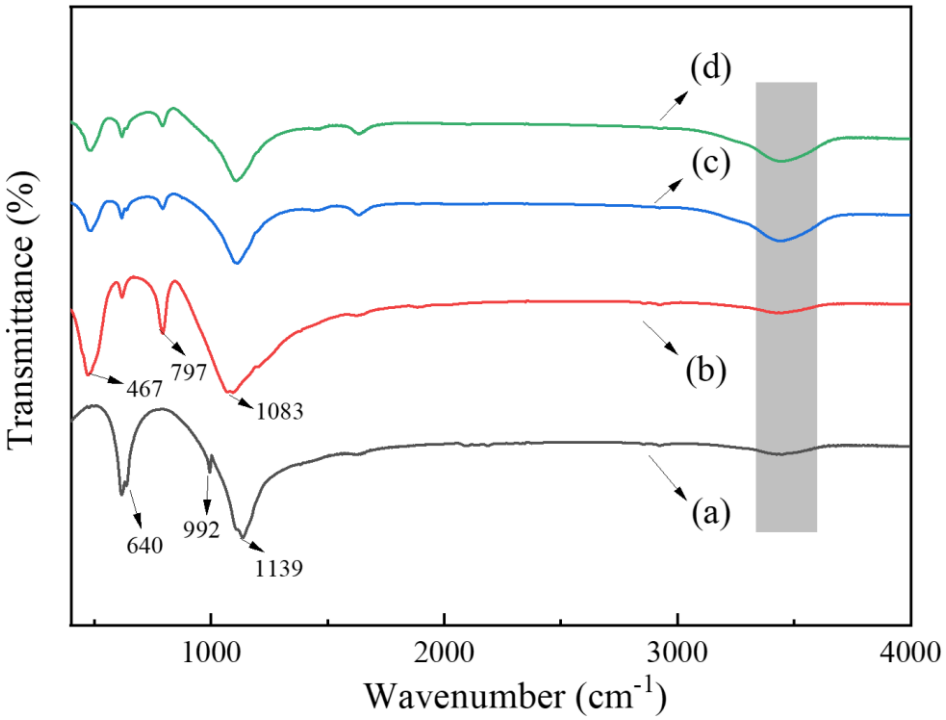

Fig. 4. FT-IR analyses for the tested samples: (a) Binary eutectic salts; (b) Diatomite; (c) Salt-diatomite composite; (d) Salt-diatomite composite after 300 thermal cycles.

3.3. Microstructural characterization

Fig. 5 (a) shows the SEM image for the salt-diatomite composite before cold sintering. It can be seen that the salt and diatomite are well mixed in the observed area after experienced mixing and compression process, in which an intact porous structure of diatomite containing plentiful pores is apparent. This cellular structure offers extra surfaces to contact the phase change liquid and hence more salt can be accommodated in the composite [8, 9]. After sintering, because of the addition of sintering liquid, there is occurrence of salt particle edge dissolution and epitaxial growth. Meanwhile, due to the solution of diatomite particle in sodium hydroxide, hydration reaction occurs between the diatomite and aqueous alkali, resulting in a distinct particle agglomeration and germination of hydroxide layer around the diatomite particles, as illustrated in Fig. 5 (b). These agglomerated diatomite particles adhere the wetted salt and encapsulate the salt surface to form a dense structure over the heating process. During such a process, a clearly sintered boundary containing a salt liquefied structure could be generated (Fig. 5 (c)), confirming the splendid wettability of diatomite towards the salt and also decent encapsulation of salt in the composite. Fig. 5 (d-f) shows the observations for the composite after 300 thermal cycles. One can see a distinctly rigid composite structure with salt being perfectly accommodated by the sintered diatomite. The micro-pores of diatomite particle existed in Fig. 5 (a) are disappeared and the size of diatomite particle seems to become smaller. This is mainly due to the taking place of salt movement in the composite structure, causing the diatomite particle being covered by molten salt over the repeated crystallization and recrystallization process.

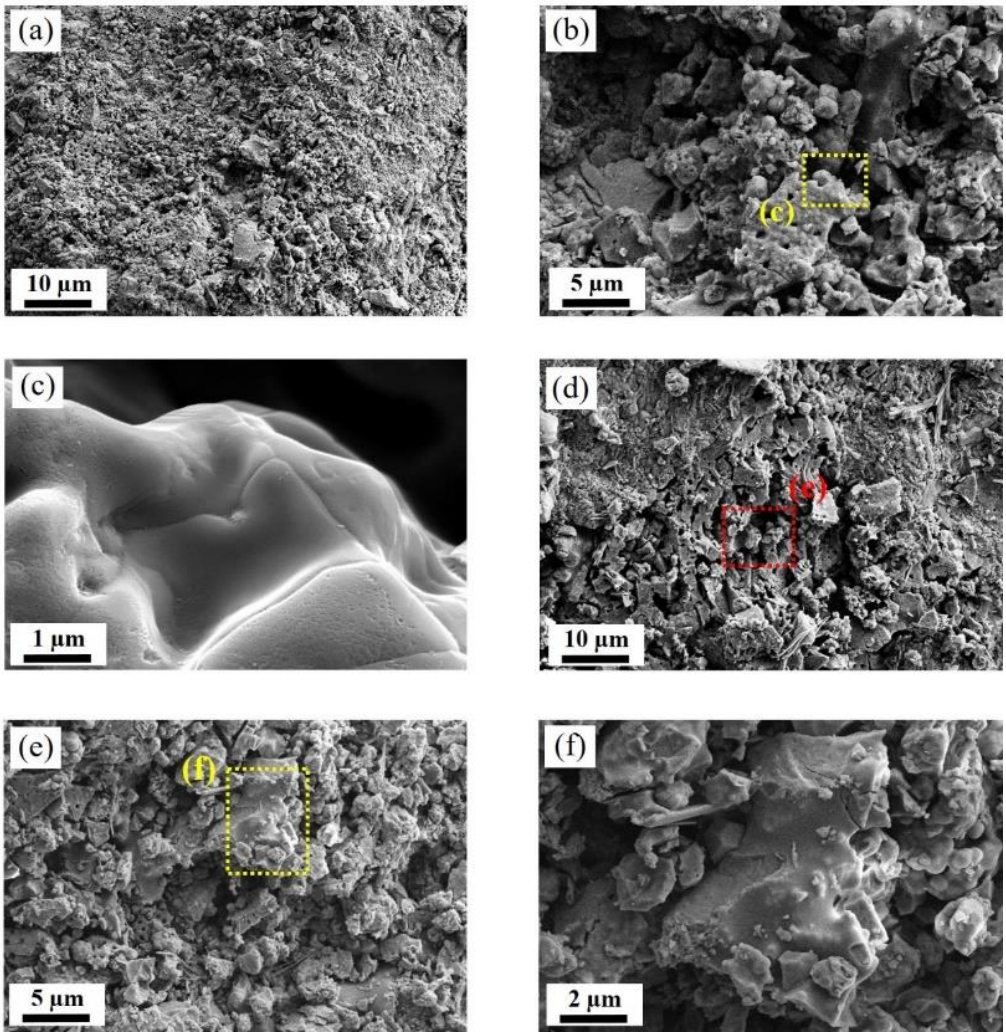

Fig. 5. SEM images of the tested samples. (a) salt-diatomite composite before sintering; (b) Salt-diatomite composite after sintering; (c) Enlarged view of the area marked in (b); (d) Salt-diatomite composite after 300 heat-cold cycles; (e) Enlarged view of the area marked in (d); (f) Enlarged view of the area marked in (e).

Fig. 6 illustrates the EDS element mapping micrographs for the composite after different thermal cycles. In the figure, the yellow colour of Si element indicates the diatomite particles distribution, while the blue colour of Na element represents the salt particles. It can be seen that after cold sintering, the salt and diatomite are distributed quite well in the composite through the particle rearrangement-precipitation process, as showed in Fig. 6 (a) and (b). The diatomite particles form a cross-bridged structure in the composite with which the salt could be effectually encapsulated and the liquid leakage could therefore be availably restricted. The generation of such a network structure is mainly attributed to the mutual solubility of salt and ceramic substance in aqueous alkali over the cold sintering process. During the particle blending stage, the adoption of sodium hydroxide solution wets and dissolves the particle surfaces of salt and diatomite, leading to the enlargement of particle contact interface and area. Owning to the hydration reaction, the Ostwald ripening and epitaxial growth are happened in the composite. After implementing compression pressure, the distances among particles are further reduced, causing the particle realignment to achieve preliminary compaction and also the liquid flow within the composite. When a sintering temperature is applied, water evaporation emerges within the composite, which accelerates the occurrence of epitaxial

precipitation, conducing to the formation of sintered network bonds among the contiguous diatomite particles to attain the final densification within the composite. Cyclic heating of composite achieves significant modifications to the element distributions. As showed in Fig. 6 (c) and (d), repeated heat and cold cycles have caused the migration and movement of the diatomite and salt to attain smaller and more uniformly distribution particles. Our previous investigations [11, 19] have demonstrated the occurrence of liquid salt movement in a salt-ceramic composite over thermal cycling process and this liquid movement could be able to pull the high interfacial energy ceramic particle movement together, leading to the particle migrations in the composite. In this work, the salt and diatomite particles are sintered by a low operation temperature that much less than the salt melting point. That is, the salt has not undergone the processes of melting and solidification. During repeated heat-cold cycles, the high cycling temperature leads to the salt phase change from solid to liquid. The liquid salt goes into the micro-spaces and cavies under a pressure discrepancy induced by volume variation and dragging force created by high interfacial energy of diatomite. Such motion results in the particle migration, promoting the redistribution of particles to achieve a more uniformly element distribution in the composite.

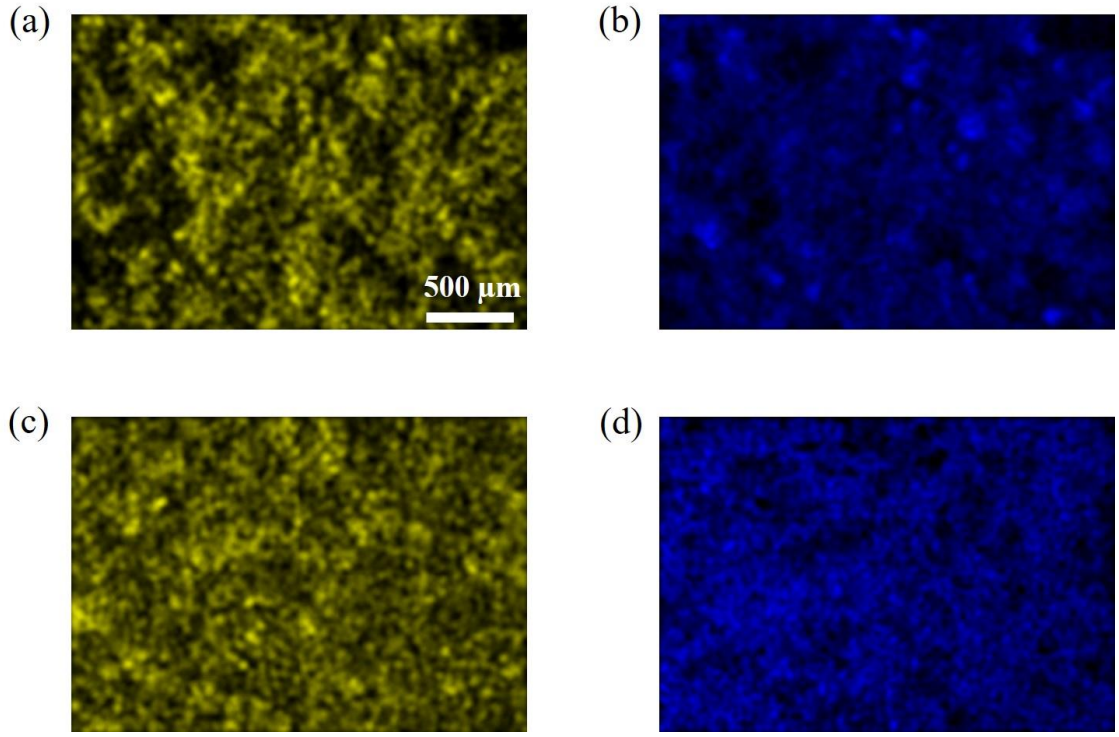

Fig. 6. (a) EDS mapping image of element Si in the composite before thermal cycling; (b) EDS mapping image of element Na in the composite before thermal cycling; (c) EDS mapping image of element Si in the composite after 300 thermal cycles; (d) EDS mapping image of element Na in the composite after 300 thermal cycles;

3.4. Mechanical property and thermal stability of the composite

In this section, the mechanical strength of the composite is explored by virtue of a universal press machine. For doing this, the salt loading ratio in the composite is kept as 60 wt.% and the test module is shaped to have a geometry dimension of 4mm in height and 12 mm in diameter. A squeeze rate of 0.2 mm/min is kept during measurement and the test will be ceased once the break or rupture of

the sample is occurred. Fig. 7 plots the measured results for the composite stress under different uniaxial pressures. It is seen that for an implemented pressure, the sample strength increases with the axial strain first and gradually decreases after reaching the maximum value. This infection point means the sample fracture moment and can be considered as the compressive strength value. As illustrated in the figure, the mechanical strength of the composite is tested as 83.88MPa, 105.87MPa and 253.84MPa when the uniaxial pressure is 150MPa, 200MPa and 250MPa, respectively. Such observation demonstrates a higher uniaxial pressure achieves a larger mechanical strength in the composite. It is worth to point out that for the given optimal uniaxial pressure of 150 MPa, the composite mechanical strength could be over 83 MPa, which is far higher than that of the sample without experiencing cold sintering where a mechanical strength of 33 MPa is observed. This substantial enhancement further demonstrates the formation of a highly densified microstructure inside the composite under the optimized cold sintering conditions. From Fig. 7, it can also be seen that a higher uniaxial pressure leads to a greater stress increasing rate of the composite, which indicates a high sintering pressure results in an increase in the Young's modulus of the composite.

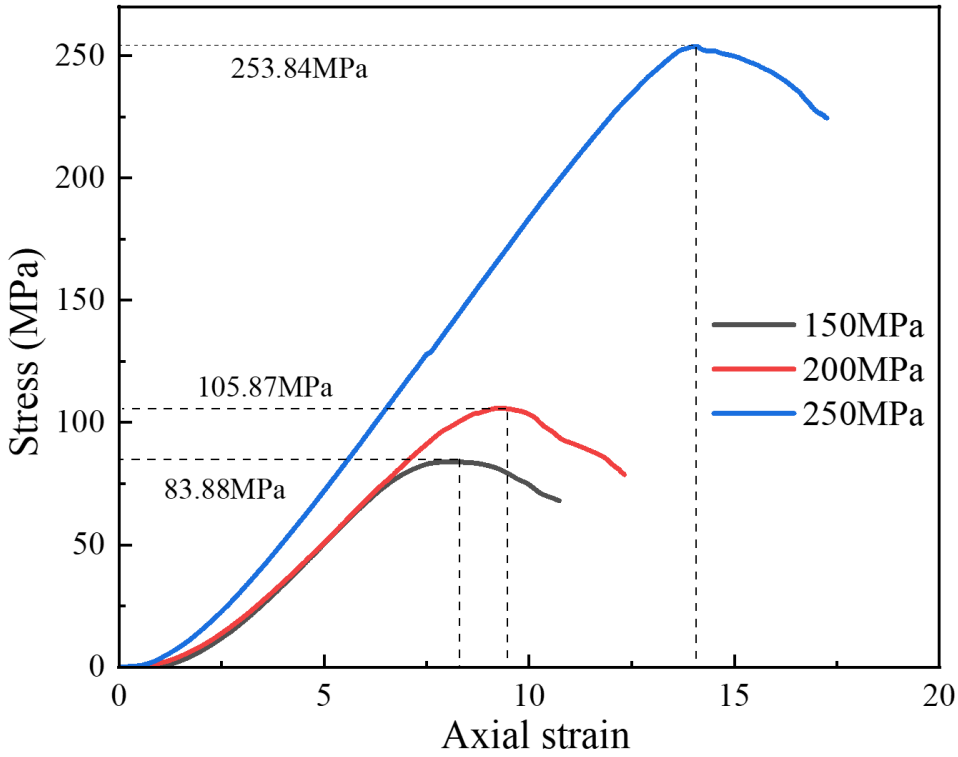

Fig. 7. Compressive strength of the salt-diatomite composite prepared under different uniaxial pressures.

The thermal stability of the composite is also examined in this section by evaluating the decomposition temperature with the use of TGA. Fig. 8 depicts the measurement results. One can see that a clear inflection point is observed for both the pure salt and composite over a temperature of 100-1000 °C, indicating the occurrence of weight loss induced by thermal decomposition. For pure sodium salt, the decomposition temperature is measured as 812.7°C. The addition of diatomite into salt to fabricate composite through cold sintering process arguments the weight loss point of pure salt. As shown in in the figure, the composite decomposition temperature is increased from 812.7°C to 865.3°C. It is noted that the thermal decomposition point of the measured sample in this work is got as the moment at which more than 3 wt.% of weight is lessened [24, 25]. The results

plotted in Fig. 8 clearly demonstrate that the composite presents a larger thermo-decomposed temperature than the sodium salt, confirming the adoption of diatomite as structure material and also the use of cold sintering technique strengthens the heat endurance of sodium salt. As mentioned above, a rigid and dense structure enriching a large number of micro-caves and pores could be generated in the composite over the particle dissolution and precipitation process. Such a structure affords space and route to accommodate the salt, which could effectively refrain the liquid phase divulge and also protect the salt from decomposition. The results shown in Fig. 8 also confirm the decent heat storage density of the composite. In consideration of the melting temperature of the composite is far less than 750 °C, it is therefore deduced that the heat storage density of the composite could be over 1000 kJ/kg at a given utilized temperature of 50-750 °C and a heat capacity of 1.19 kJ/kg·°C.

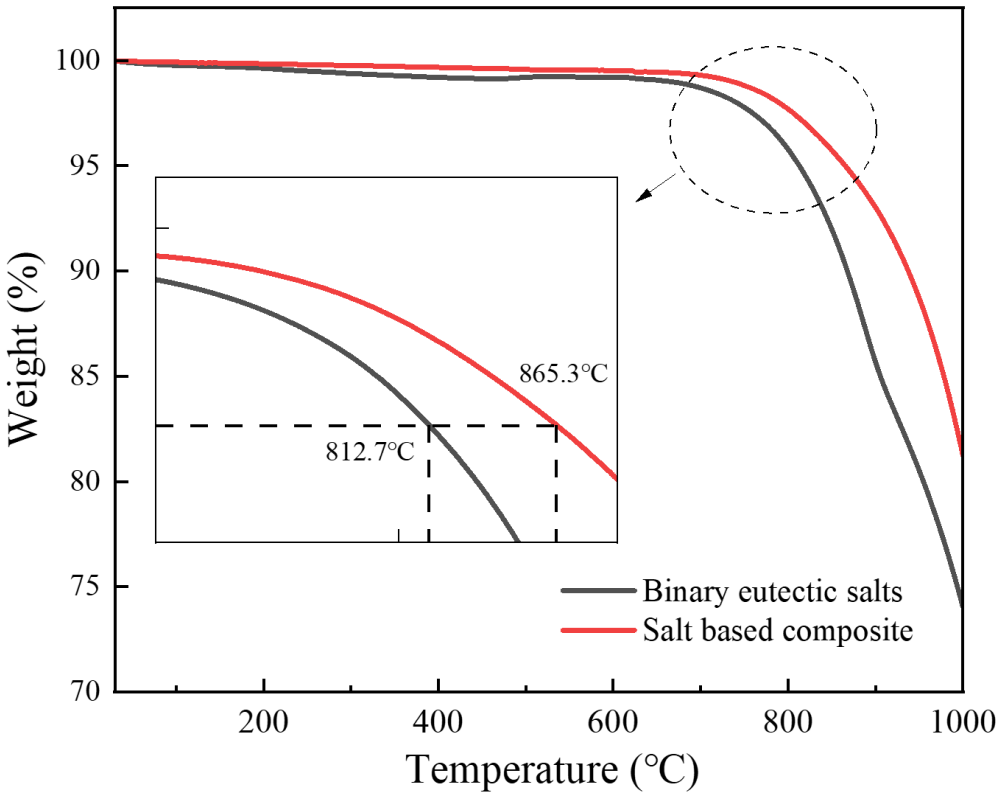

Fig. 8. TG measurements for the pure salt and salt-diatomite composite.

3.5. Phase change behaviour and thermal energy storage performance

Fig. 9 shows the DSC curves for the salt-diatomite composite. For comparison purpose, the curve for the pure sodium salt is also given in the figure. It can be seen that after cold sintering process, the composite achieves a melting point of 623.9 °C and a latent heat of 148.2 kJ/kg. This indicates the composite developed in this investigation could be a competitive candidate used in high-temperature heat energy storage domains. In comparison with the sodium salt where a melting temperature of 622.9 °C and a latent heat of 240.5 kJ/kg observed, the addition of diatomite brings down the salt enthalpy and also shift the sample phase change temperature. The reason for the enthalpy variation is mainly attributed to the salt concentration reduction. For the tested sample, the salt loading ratio is kept as 60 wt.% and thus a lessened latent heat is obtained in the composite compared to the sodium salt. On the other hand, the enthalpy ratio of composite to pure sodium salt

is calculated as 61%, which is close to the theoretical value of salt enthalpy in the composite, confirming the decent encapsulation of liquid salt and also a rigid structure formed over the cold sintering process. The shift of melting temperature could be related to the physical interaction between the diatomite and salt. Goitandia et al. [27] and Nomura et al. [28] have indicated that the confinement impact of porous structure on the PCM phase change behaviour and hence a minor alteration of melting temperature is observed over the measurement process. Shown in Fig. 9 also finds the DSC curve for the sample experienced 300 thermal cycles. One can see a fluctuation of latent heat value and melting temperature. The un-encapsulated phase change substance at the outer surface of the composite is the main reason for this observation. To figure out the detailed relationship between the cycling times and sample phase change behaviour, more than 300 times of thermal cycling have been performed and the results are plotted in Fig. 10. One can see that with the thermal cycle evolves, the most serious leakage occurs in the sample experienced 150 thermal cycles and after that, the trend of reduction becomes gradually less. At 300 heating-cooling cycles, there is almost no liquid leakage appeared in the composite. This is because that the un-coated salt becomes less caused by leakage with the increase of thermal cycle times and hence a stable composite without divulgence will be achieved. After experienced 300 thermal cycles, the latent heat of the sample decreases by 4.9% from 148.2 kJ/kg to 140.8 kJ/kg. Such reduction is similar with the situations reported in the literatures [23, 24] and the main reason could be attributed to the liquid phase leakage at the apparent surface where a fraction of salt is not properly encapsulated. This is evidenced by the fact that the degree of decrease in salt mass becomes less strong because the un-accommodated salt located at outer surface cuts down gradually with the progress of thermal cycles. From the 150 heat cycles to 300 heat cycles, it only has less than 1.8% reduction in the latent heat.

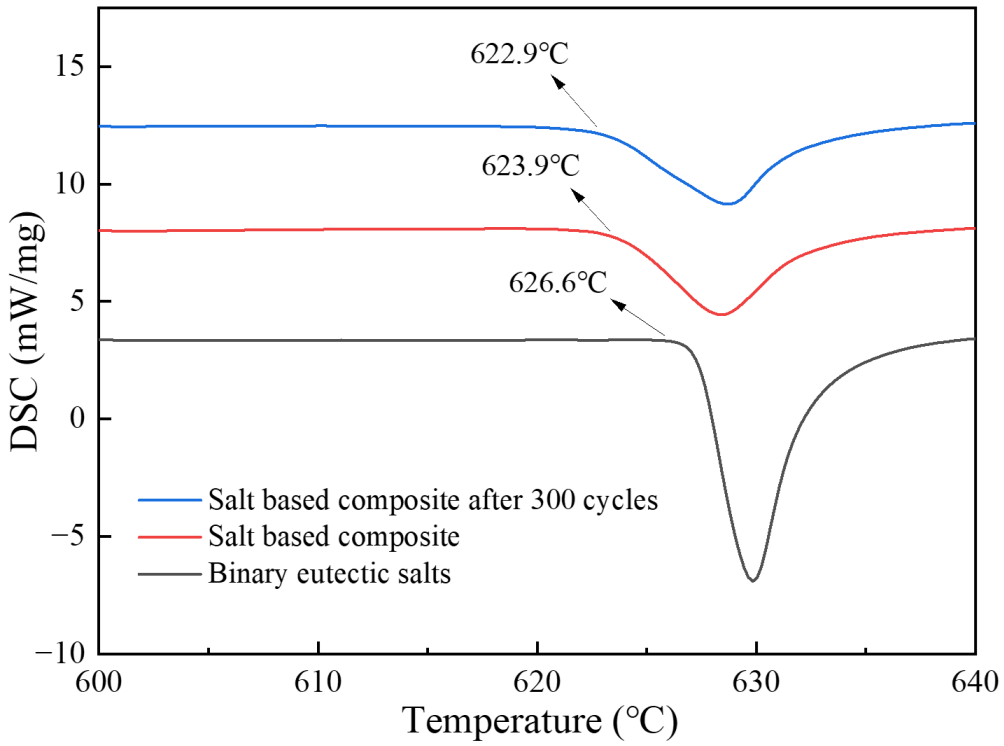

Fig. 9. DSC curves of the pure binary eutectic salt and salt-diatomite composite after different thermal cycles.

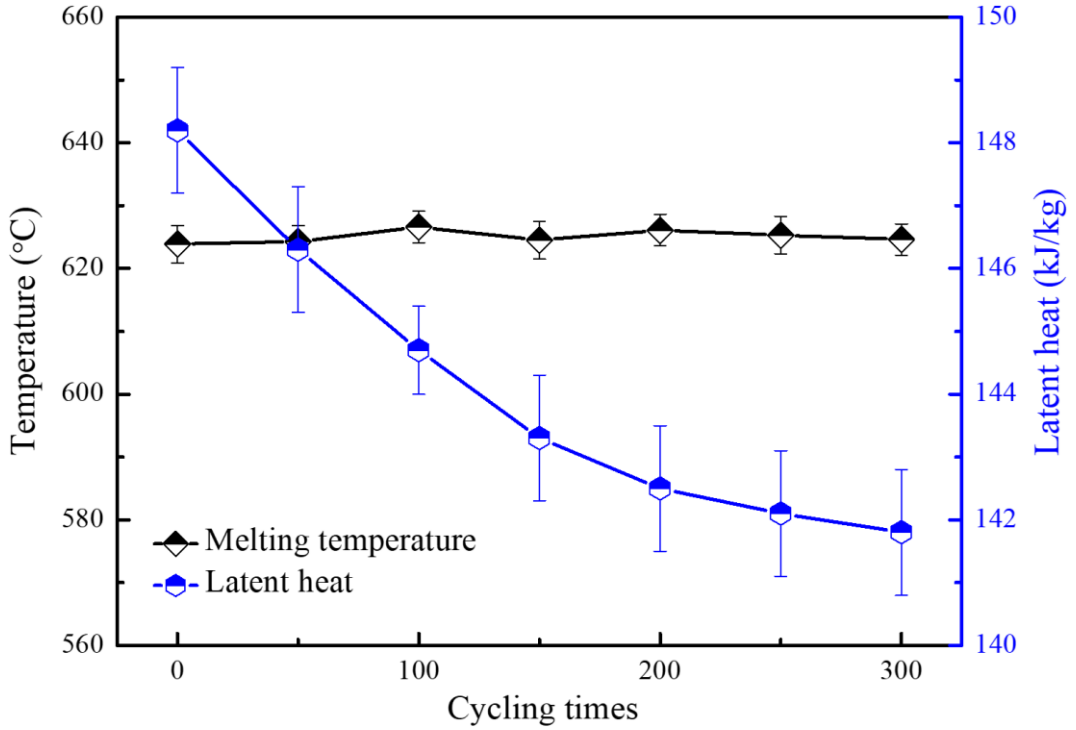

Fig. 10. Variations of composite melting temperature and latent heat with thermal cycling times.

Table 1 summarizes the comparison of previous investigations on the salt composites with the present work. It can be seen that the composite developed in this work achieves a relatively high latent heat and salt loading ratio. Compared to other samples where a high sintering temperature typically larger than the melting point is required, an ultra-low sintering temperature as little as 150 °C is observed in the sodium salt based composite, which confirms the fabrication feasibility of a high melting point salt composite by a low sintering temperature with cold sintering approach and the superiority of current composite in the high temperature thermal energy storage fields.

Table 1 Comparison of previous investigations with the present work

Composites	Salt ratio (wt%)	Composition ratio (wt%)	T_m (°C)	H (J/g)	Sintering Temp. (°C)	Refs.
KNO_3-diatomite	-	65-35	330	60.52	380	[10]
NaCl/KCl/$MgCl_2$-porous SiC	23-14-63	50-50	385	131.5	450	[15]
NaCl/KCl/$MgCl_2$-MgO-EG	51-22-27	45-40-15	386	81.1	450	[18]
K_2CO_3/Li_2CO_3/Na_2CO_3-MgO	44-23-33	50-50	386	158.7	450	[16]
NaCl/KCl/$MgCl_2$-EG-SiO_2	14-17.8-68.2	69-30-1	382	123.7	450	[14]
Li_2CO_3/Na_2CO_3-MgO-graphite	43-57	45-45-10	498	178.3	550	[11]

Na_2CO_3/NaCl-mullite-SiC	59.45-40.55	48-32-20	646	151	700	[13]
NaCl/KCl-modified steel slag	43.5-56.5	50-50	653	139	700	[13]
NaCl/Na_2SO_4-Diatomite	32-68	60-40	623.9	148.2	150	This work

The thermal energy storage performance of the composite containing different mass concentration of salt is also investigated in this section by exploring the sample charging and discharging behaviours at varied conditions. For doing so, a self-designed heat transfer platform involving a heating unit and a data record module is adopted to monitor the temperature variations within the composite. A cylindrical sample with a size of 50 mm in diameter and 5 mm in height is fabricated and employed for testing. Over the charging process, the sample glued with thermal conductive silicone is placed in the heating platform and the periphery is covered by vermiculite insulation board. The heating unit temperature is set as 660 °C and a K-type thermocouple is inserted into the central position of the composite for temperature monitoring. The heating process is regarded as complete when a preset temperature of 660 °C is achieved; at this point, the power of the heating unit is switched off and discharging process starts with all covers of the composite being dislodged to allow the sample cool down under an electric fan. Fig. 11 plots the curves on the measured temperature fluctuation with time inside the composite. One can see that for charging process illustrated in Fig. 11 (a), a three-stage heat storage process is apparent: a sensible heat storage zone (Stage I), a latent heat storage zone (Stage II) and a sensible heat storage zone (Stage III). The stage I lasts between ~500 s and ~1500 s, and the duration is mainly depended on the composite effective thermal conductivity; the larger concentration of salt, the higher thermal conductivity and hence the faster heat transfer rate in the composite. The occurrence of Stage II is due to phase transition of sodium salt in the composite and the process sustains between ~500 s and ~1800 s. This result is in line with the DSC data showed in Fig. 9 that a higher concentration of salt leads to a larger latent heat in the composite and hence a longer phase transition observed over the measurement. For Stage III, the continue rising of temperature is because of sensible heat storage of liquid sodium salt in which a fast heat transfer rate is observed. From Fig. 11 (a), one can also see that different mass ratio of salt and skeleton supporting material achieves an apparent heat transfer difference in the composite. For the composite containing a high concentration of salt, the heat transfer rate is clearly higher than other samples. When the salt concentration is augmented from 80 wt.% to 60 wt.%, the heat transfer duration can be shortened by 56.1% decreasing from 4100 s to 1800 s. This is in agreement with the results on the thermal conductivity measurements in which a high mass ratio of salt achieves a large thermal conductivity of the composite. Other reason for such observation lies in the decrease of heat storage density. In a composite containing a PCM, the major heat is stored through the form of latent heat. A larger loading of salt means a lower concentration of diatomite and thus a lower heat storage capacity and a fast heat storage process within the composite. The discharging process presented in Fig. 11 (b) also exhibits a three-stage characteristic. Similar to the charging process, the composite containing 60 wt.% salt achieves the fastest heat release rate under the given working conditions. For the measuring temperature decreasing from 660 °C to 277 °C, it only takes ~6500 s for the composite with 60 wt.% salt, which is reduced by 35% compared to the composite containing 80 wt.% diatomite where a duration of ~10000 s is needed. Fig. 11 (b) also

presents that the improvement in heat transfer rate induced by the increase of salt is gradually decreased when the salt concentration increases from 20 wt.% to 60 wt.%, indicating there exists an optimal mass loading of salt in the composite and further increase salt concentration has no influence on the heat transfer rate. As discussed above, an increase of diatomite indicates a stable structure in the composite and hence the right balance among the concentration of components must be attained in the composite for achieving a decent integration of effective thermal conductivity and heat storage density. The doping of thermal conductivity enhancer into composite seems to be a good solution for this and the implement of such strategy boned with cold sintering technique will be carried out in our further experiments. This observation together with the results showed in Fig. 10 and Fig. 11 demonstrate a splendid cycling performance and thermal energy storage behaviour achieved in the salt-diatomite composite.

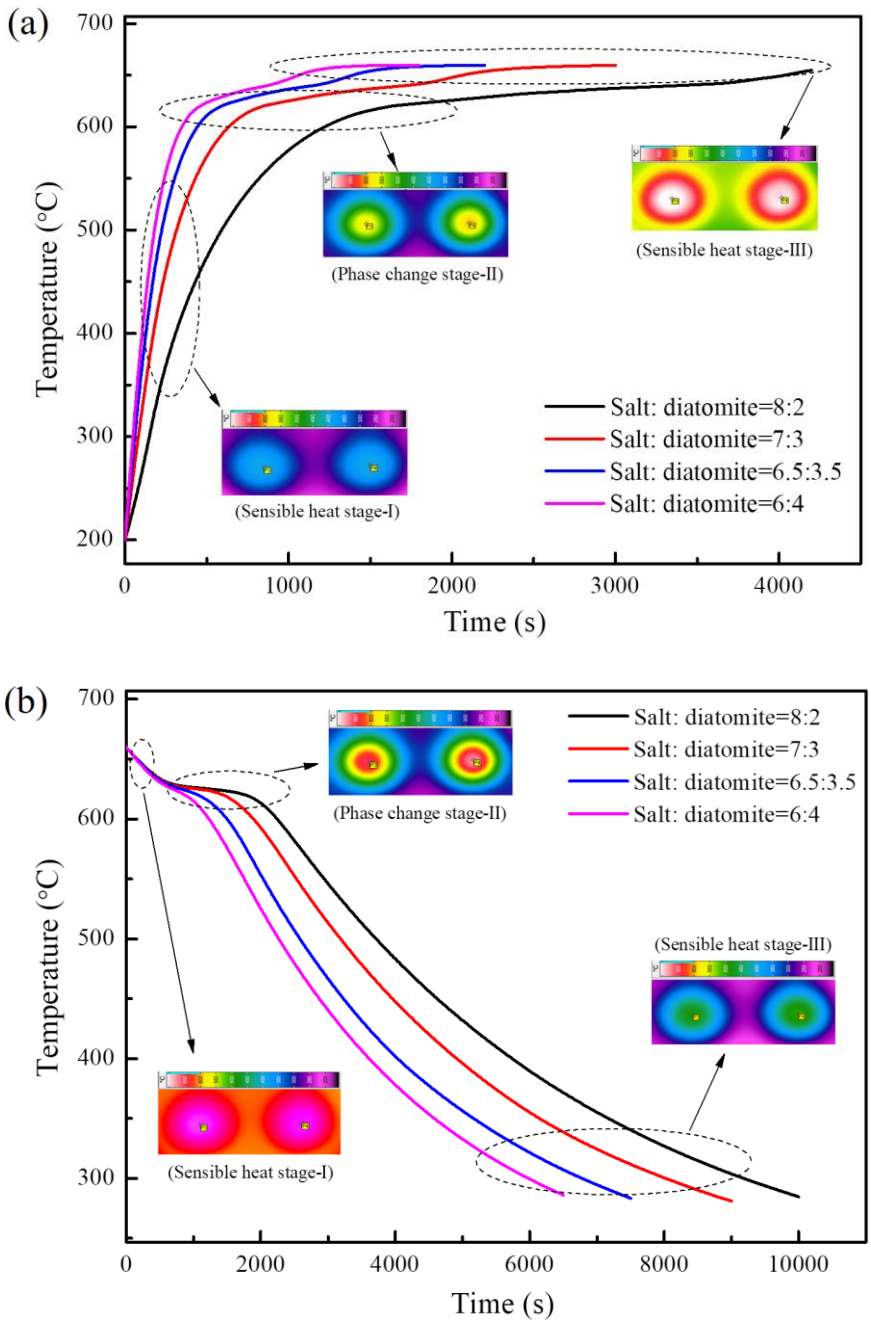

Fig. 11. Thermal energy storage performance of the salt-diatomite composite over the charging (a) and discharging (b) processes.; The insert images show the corresponding IR observations on the composite at different charging and discharging stages.

4. Conclusions

A high melting point binary sodium salt composite suited for high-temperature thermal energy storage is developed and evaluated in this work. A novel cold sintering approach is adopted for the material preparation with the employment of diatomite as ceramic supporting skeleton and aqueous alkali as sintering liquid. The following conclusions could be gained:

(1) The composite could be successfully fabricated by an ultra-low sintering temperature as little as 150 °C. By employing aqueous alkali as sintering additive, a shape-stabilized framework containing a compact and dense microstructure could be obtained in the composite.

(2) An outstanding chemical and physical compatibility is achieved in the composite. Due to mutual solution of salt and diatomite in sodium hydroxide solution, a cross-linking network microstructure is generated, which could effectually accommodate the salt and restrain the liquid divulge over the repeated heating-cooling cycles.

(3) Over 60% of salt could be encapsulated in the composite with the adoption of diatomite as ceramic skeleton. In this mass ratio, a melting temperature of 623.9 °C and a latent heat of 148.2 kJ/kg could be attained in the composite. For a given utilized temperature of 50-750 °C, the composite heat storage density could be over 1000 kJ/kg.

(4) At a given cold sintering uniaxial pressure of 250MPa, a mechanical strength as high as 253.84MPa could be achieved in the composite. Moreover, the composite presents excellent cycling performance. After experienced 300 heat-cold cycles, the composite latent heat and melting point only varies 4.9% and 1.2% decreasing to 140.8kJ/kg and 622.9 °C, respectively.

Acknowledgements

The work was supported by the National Key Research and Development Program of China (2025YFE0121000) and National Natural Science Foundation of China (52406214).

References

[1] Saliha Saher, Sam Johnston, Ratu Esther-Kelvin, Jennifer M. Pringle, Douglas R. Macfarlane, Karolina Matuszek. Trimodal thermal energy storage material for renewable energy applications. Nature 636 (2024) 622-626.

[2] Jason Woods, Allison Mahvi, Anurag Goyal, Eric Kozubal, Adewale Odukomaiya, Roderic Jackson. Rate capability and Ragone plots for phase change thermal energy storage. Nature Energy 6 (2021) 295-302.

[3] Sheng Yang, Hong-Yi Shi, Jia Liu, Yang-Yan Lai, Ozgur Bayer, Li-Wu Fan. Supercooled erythritol for high-performance seasonal thermal energy storage. Nature Communications 15 (2024) 4948.

[4] Ekaterina Pomerantseva, Francesco Bonaccorso, Xinliang Feng, Yi Cui, Yury Gogotsi. Energy storage: The future enabled by nanomaterials. Science 366 (2019) 6468.

[5] Lin-kui Feng, Yao-fei Feng, Ke Lu, Ping Wang, Kai Zhao, Zhi-de Gu, Yan-nan Ren, Sheng-lu Xie. The analysis of molten salt energy storage mode with multi-steam sources heating in thermal power unit peak shaving operation. Scientific Reports 15 (2025) 11305.

[6] Xinyu Huang, Muzhi Li, Yuanji Li, Xiaohu Yang, Ya-Ling He. Current progress in energy utilization of building systems combining solar thermal and heat storage technologies. Renewable and Sustainable Energy Reviews 226 (2026) 116330.

[7] Zhenyu Cao, Shiyu Sun, Guihua Ma, Anyu Feng, Kang Kang, Guotao Sun, Jianming Li. Phase change materials for efficient thermal energy storage and its potential applications in sustainable facility agriculture: A critical review. Renewable and Sustainable Energy Reviews 225 (2026) 116169.

[8] Naveen Jose, Menon Rekha Ravindra. Microencapsulation approaches for the development of novel thermal energy storage systems and their applications. Solar Energy Materials and Solar Cells 280 (2025) 113271.

[9] Yingying Tian, Ruiying Yang, Haokun Pan, Nannan Zheng, Xiubing Huang. Biomass-based shape-stabilized phase change materials for thermal energy storage and multiple energy conversion. Nano Energy 133 (2025) 110440.

[10] Qi Li, Chuan Li, Zheng Du, Feng Jiang, Yulong Ding. A review of performance investigation and enhancement of shell and tube thermal energy storage device containing molten salt based phase change materials for medium and high temperature applications. Applied Energy 255 (2019) 113806.

[11] Chuan Li, Qi Li, Lin Cong, Feng Jiang, Yanqi Zhao, Chuanping Liu, Yaxuan Xiong, Chun Chang, Yulong Ding. Mgo based composite phase change materials for thermal energy storage: The effects of MgO particle density and size on microstructural characteristics as well as thermophysical and mechanical properties. Applied Energy 250 (2019) 81-91.

[12] Qi Li, Lin Cong, Xusheng Zhang, Bo Dong, Boyang Zou, Zheng Du, Yaxuan Xiong, Chuan Li. Fabrication and thermal properties investigation of aluminium based composite phase change material for medium and high temperature thermal energy storage. Solar Energy Materials and Solar Cells 211 (2020) 110511.

[13] Chuan Li, Qi Li, Ruihuan Ge. A review of heat transfer performance enhancement and applications of inorganic salt based shape-stabilized composite phase change materials for medium and high temperature thermal energy storage. Energy Reports 8 (2022) 12740-12764.

[14] Ziyuan Li, Yangjun Wang, Huan Wang, Shuai Zhang, Zhen Shang, Limei Tian, Yuying Yan. Enhancing the thermal cyclic reliability of salt-based shape-stabilized phase change materials by in-situ SiO_2-C interconnectivity in rice husk carbon. Journal of Cleaner Production 466 (2024) 142864.

[15] Xiaoyan Yao, Yunwei Chang, Heng Gu, Jiangrong Guo, Deqiu Zou. Preparation and thermophysical properties of a novel metallic microencapsulated phase change material/eutectic salt/ceramic composite. Chemical Engineering Journal 477 (2023) 146967.

[16] Xiaoyan Yao, Chenwu Shi, Shuyan Zhu, Binghui Wang, Wang Hao, Deqiu Zou. Thermal

performance enhancement of ceramics based thermal energy storage composites containing inorganic slat/metallic micro-encapsulated phase change material. Solar Energy Materials and Solar Cells 288 (2025) 113645.

[17] Xuhao Liu, Hao Liu, Zhoufu Wang, Wenyuan Liu, Yan Ma, Zhenghuang Quan, Xitang Wang. Effects of particle packing structure on molten salts migration behaviour and thermal properties in composite phase change materials. Solar Energy 301 (2025) 113922.

[18] Chuan Li, Haitao Lu, Qi Li, Rongyu Xu, Zhigang Liu, Yi Yang, Shi Liu, Yuting Wu. Fabrication and investigation of chloride salt based shape stabilization phase change composite with excellent thermal properties for medium and high temperature thermal energy storage. Solar Energy Materials and Solar Cells 278 (2024) 113200.

[19] Chuan Li, Li Han, Qi Li, Guoyun Leng, Haitao Lu, Rongyu Xu, Yanping Du, Yuting Wu. Development and investigation of salt based composite phase change material containing diatomite as skeleton substance by cold sintering technology for medium and high temperature thermal energy storage. Solar Energy Materials and Solar Cells 271 (2024) 112821.

[20] Chuan Li, Li Han, Qi Li, Yanping Du, Yuting Wu. Preparation and densification behaviour of magnesia-nitrate salt composite phase change material fabricated by cold sintering technology for thermal energy storage. Journal of Thermal Science 34 (2025) 970-981.

[21] Ning Guo, Ming Liu, Jie-Yu Shen, Hui-Zhen Shen, Ping Shen, Surface hydrate-assisted low- and medium-temperature sintering of MgO. Scripta Materialia 206 (2022) 114258.

[22] Keitaro Yamaguchi, Shinobu Hashimoto. Mechanism of densification of calcium carbonate by cold sintering process. Journal of the European Ceramic Society 42 (2022) 6048-6055.

[23] Qinghua Yu, Zhu Jiang, Lin Cong, Tiejun Lu, Bilyaminu Suleiman, Guanghui Leng, Zhentao Wu, Yulong Ding, Yongliang Li. A novel low-temperature fabrication approach of composite phase change materials for high temperature thermal energy storage. Applied Energy 237 (2019) 367-377.

[24] Bilyaminu Suleiman, Qinghua Yu, Yulong Ding, Yongliang Li. Fabrication of form stable NaCl-Al_2O_3 composite for thermal energy storage by cold sintering process. Frontiers of Chemical Science and Engineering 13 (2019) 727-735.

[25] Ming Liu, Quan Jin, Ping Shen. Cold sintering of $NaNO_3$/MgO heat-storage composite. Ceramics International 46 (2020) 28955-28960.

[26] Kaoutar Moulakhnif, Abdelkoddouss El Majd, Hanane Ait Ousaleh, Abdessamad Faik, Said Sair, Abdeslam El Bouari. Thermal performance of shape-stable hydrated salt-based modified diatomite composite phase change materials for low-temperature heat storage. Solar Energy Materials and Solar Cells 294 (2026) 113935.

[27] Amaia M. Goitandia, Garikoitz Beobide, Estibaliz Aranzabe, Ana Aranzabe. Development of content-stable phase change composites by infiltration into inorganic porous supports. Solar Energy Materials and Solar Cells 134 (2015) 318-328.

[28] Takahiro Nomura, Noriyuki Okinaka, Tomohiro Akiyama. Impregnation of porous material with phase change material for thermal energy storage. Materials Chemistry and Physics 115 (2009) 846-850.